Molecular mechanism of water oxidation in photosynthesis based on the functioning of manganese in two different environments

(oxygen evolution/model/manganese–quinone complex/electron transfer)

T. KAMBARA* AND GOVINDJEE[†]

Departments of Physiology and Biophysics, and Plant Biology, University of Illinois at Urbana-Champaign, 289 Morrill Hall, 505 South Goodwin Avenue, Urbana, IL 61801

ABSTRACT   We present a model of photosynthetic water oxidation that utilizes the property of higher-valent Mn ions in two different environments and the characteristic function of redox-active ligands to explain all known aspects of electron transfer from H_2O to Z, the electron donor to P680, the photosystem II reaction center chlorophyll *a*. There are two major features of this model. (*i*) The four functional Mn atoms are divided into two groups of two Mn each: [Mn] complexes in a hydrophobic cavity in the intrinsic 34-kDa protein; and (Mn) complexes on the hydrophilic surface of the extrinsic 33-kDa protein. The oxidation of H_2O is carried out by two [Mn] complexes, and the protons are transferred from a [Mn] complex to a (Mn) complex along the hydrogen bond between their respective ligand H_2O molecules. (*ii*) Each of the two [Mn] ions binds one redox-active ligand (RAL), such as a quinone (alternatively, an aromatic amino acid residue). Electron transfer occurs from the reduced RAL to the oxidized Z. When the experimental data concerning atomic structure of the water-oxidizing center (WOC), electron transfer between the WOC and Z, the electronic structure of the WOC, the proton-release pattern, and the effect of Cl^- are compared with the predictions of the model, satisfactory qualitative and, in many instances, quantitative agreements are obtained. In particular, this model clarifies the origin of the observed absorption-difference spectra, which have the same pattern in all S-state transitions, and of the effect of Cl^--depletion on the S states.

Oxidation of water to molecular oxygen is carried out in plants through a four-step univalent redox sequence promoted by photo-induced oxidation of the photosystem II (PSII) reaction center P680 (for reviews, see refs. 1 and 2). An electron carrier Z, which exists between the water oxidation center (WOC) and P680, is suggested to be a bound plastoquinol PQH_2 (3); Mn ions are included in the WOC and play an essential role in the H_2O oxidation process (for review, see ref. 4); cooperation of several intrinsic and extrinsic polypeptides is required for the functioning of Mn (1); and chloride ions are also essential (5). However, the mechanism of H_2O oxidation is not understood in its details and further studies are required. Various models have been proposed (6–11) that suggest how the state of the WOC, described in terms of the redox state of Mn ions and the chemical forms of the intermediates of H_2O oxidation, are changed during the four-step univalent redox sequence according to Kok's four-photon scheme (2). However, none of the earlier models explains all of the existing data, and no laboratory has yet succeeded in revealing unequivocally the microscopic structure of the WOC. We present here a model for the mechanism of H_2O oxidation in photosynthetic systems. It utilizes the chemistry of higher-valency Mn ions

in two different environments and the characteristic function of redox-active ligands to explain all known aspects of electron transfer from H_2O to Z and to provide a possible explanation for the mechanism of H_2O splitting. Predictions based on this model are consistent with the various observed data.

THE MODEL

Basic Assumptions of the Model

1. The WOC consists of two main parts (Fig. 1): two Mn complexes in a hydrophobic cavity of the 34-kDa intrinsic polypeptide (referred to as [Mn]) and two Mn complexes on the hydrophilic surface of the 33-kDa extrinsic protein [referred to as (Mn)].

2. Each of the two [Mn] ions binds one redox-active ligand (RAL), such as a quinone or an aromatic amino acid residue.

3. Electron transfer occurs from the reduced RAL in a [Mn] complex to Z^+. Structural conditions favor the electron transfer from RAL to Z^+ in one complex (complex A, designated A-[Mn]) as compared with the other (complex B, designated B-[Mn]).

4. The hydrophobic cavity of the intrinsic 34-kDa protein accommodates only two H_2O molecules, each of which is bound directly to a [Mn] ion.

5. The (Mn) complex is surrounded by the intrinsic 34-kDa and extrinsic 33-kDa proteins and is similar to a Mn^{3+} complex in aqueous media.

6. Cl^-, present in the hydrophilic region, coordinate to (Mn) ions indirectly as outer-sphere ligands in order to stabilize the trivalent (Mn) ions.

7. Each of the two (Mn) complexes is bound to one of the two [Mn] complexes through a hydrogen bond between their respective ligand H_2O molecules. The protons released from the two H_2O molecules that are bound to the [Mn] complexes are transferred to the (Mn) complexes along the hydrogen bond.

Justification of the Assumptions

Assumption 1: Heterogeneity of Mn. Many workers (1, 12–15) have concluded that there are four functional Mn atoms in the WOC; these are divided into two groups of two Mn each, and Mn atoms in one group are more loosely bound

---

Abbreviations: [Mn], Mn ion in a hydrophobic cavity in the intrinsic 34-kDa protein; (Mn), Mn ion on the hydrophilic surface of the extrinsic 33-kDa protein; PSII, photosystem II; P680, PSII reaction center chlorophyll *a*; RAL, redox-active ligand; S_n, state of the oxygen-evolving system; WOC, water oxidation center; Z, electron donor to P680$^+$; PQ, plastoquinol; XAES, x-ray absorption edge spectra.
*Permanent address: Department of Engineering Physics, University of Electro-Communications, Chofu, Tokyo, 182 Japan.
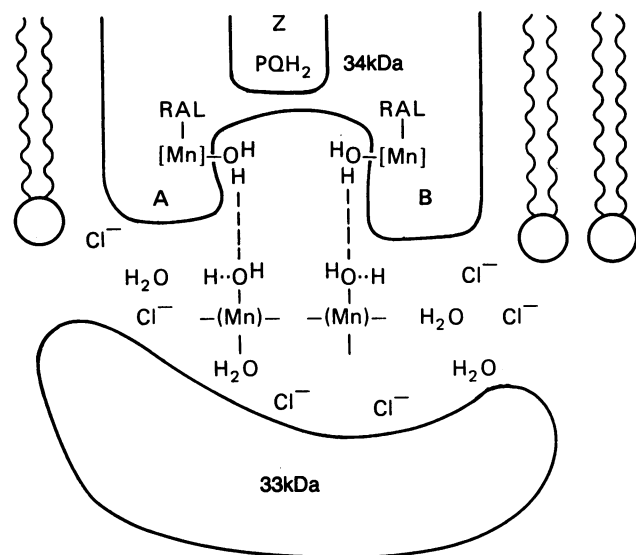[†]To whom reprint requests should be addressed.

FIG. 1. Model of the structural organization of the WOC. [Mn] and (Mn), Mn ions in the hydrophobic cavity and in the hydrophilic region, respectively; 34-kDa and 33-kDa, the intrinsic and extrinsic polypeptides, respectively; Z, electron donor to P680; dashed lines, hydrogen bonds. A H_2O ligand of (Mn) ion is denoted as HO··H in order to show the equilibrium state of $(Mn)OH_2 \rightleftarrows (Mn)OH^- + H^+$ in the hydrophilic region. The two [Mn] complexes are distinguished by symbols A and B.

to the WOC than those in the other group. Metz *et al.* (16) have shown the existence of an intrinsic 34-kDa protein whose absence is correlated with the loss of O_2 evolution and a decrease in the amount of bound Mn atoms. Miyao and Murata (17) have found that diminished O_2 evolution is correlated with the release of the extrinsic 33-kDa protein. Assumption 1 is derived from the following consideration based on the above observations: H_2O oxidation must be carried out under conditions where the reactive intermediates of H_2O oxidation are physically protected by separation from other molecules. On the other hand, in order for the reaction to proceed, the system must continuously take up H_2O molecules and release protons and O_2 molecules. Therefore, the reaction site is required to readily equilibrate with the inner aqueous space of grana. The structure of our model (Fig. 1) satisfies these seemingly contradictory conditions.

Assumption 2: RAL. We do not know the nature of the ions or molecules that ligate with the functional Mn atoms (1). We have assumed a structure for the [Mn] complex consistent with the data of biomimetic complexes. The [Mn]–RAL complex acts as the charge accumulation center of the WOC and brings two O atoms into close enough proximity to form an O—O bond. Mn–catechol complexes have these properties (18, 19).

Assumption 3: Electron Flow to Z^+. The microscopic process of electron transfer from the WOC to Z^+ is poorly understood. However, Z^+ is probably PQH_2^+ (3, 20). Also, a close interaction is known to exist between Mn and Z (21, 22). Therefore, we have estimated the electron transfer path from Mn to Z^+ based on these facts and the existing data about oxidation of Mn in Mn(II)-di-*tert*-butylcatechol mixture in perchlorate solution (18). The assumption about the unequivalence of the A- and B-[Mn] complexes is made to allow the sequential oxidation of the two [Mn] complexes.

Assumption 4: Two H_2O Molecules. We do not yet know whether H_2O molecules are bound to the functional Mn atoms directly or indirectly. The biomimetic Mn complexes coordinate H_2O molecules directly to Mn atoms (8). In a Mn superoxide dismutase protein, one H_2O molecule coordinates

directly to the Mn(III) ion (23). From the cleft size of $\approx 4 \times 2.5$ Å (24), only two H_2O molecules would be bound at a time.

Assumptions 5 and 6: Environment of Hydrophilic Mn. Seibert and Cotton (25) have shown that loosely bound Mn atoms are located between the 33-kDa extrinsic protein and the PSII membrane, presumably at the site of the 34-kDa intrinsic polypeptide. Since the thylakoid lumen is an aqueous environment, assumption 5 seems quite reasonable except for the fact that the Mn ion is trivalent. Mn^{3+} is a strong oxidant, unstable in aqueous media; it is, however, stable in dilute perchlorate solution (26). The unique property of Mn^{3+} in its reaction with H_2O is that the equilibrium constant in the reaction: $Mn^{3+}(H_2O) + H_2O \rightleftarrows Mn^{3+}(OH)^- + H_3O^+$ is extremely large (≈ 0.9, ref. 27). The role of Cl^- as a stabilizer of Mn^{3+} is straightforward.

Assumption 7: Arrangements of Two Different Mn Complexes. It is still unclear how the two groups of functional Mn atoms couple with each other. We suggest that the [Mn] complex carries out the oxidation of H_2O and the (Mn) complex assists the oxidation by pulling away H_2O protons along the hydrogen bond and releasing them into the lumen. Such a proton transfer through a hydrogen bond is one of the common mechanisms for proton translocation in biological systems (28). Therefore, assumption 7 is reasonable.

Mechanism of H_2O Splitting

The microscopic mechanism of electron transfer and H_2O splitting in photosynthesis is described by Kok's four-photon scheme of the redox cycle ($S_0 \rightarrow S_1 \rightarrow S_2 \rightarrow S_3 \rightarrow S_4 \rightarrow S_0$, where S_n represents the redox state of the WOC). The essence of this mechanism is shown schematically in Fig. 2.

Electron Transfer Process from the WOC to Z^+. The electron transfer from the WOC to Z^+ occurs through a RAL. The electron transfer to Z^+ takes place first from the A-[Mn] complex and only later from B-[Mn].

The Process for the $S_0 \rightarrow S_1$ Reaction. $S_0 \rightarrow S_1'$. After the absorption of a photon by P680 and the production of Z^+, an electron is transferred from RAL in A-[Mn] to Z^+: RAL^+ is formed. The midpoint potential of the Z/Z^+ redox couple is about $+1.0$ V (29). The oxidation potential of catechol (Cat) in the reaction $Mn^{3+}(Cat)_3 \rightarrow Mn^{3+}(Cat)_2(SQ) + e^-$ (where SQ = semiquinone) is $+0.44$ V in aprotic media (8). Thus, if RAL is a catechol, the [Mn(III)]–RAL complex may be oxidized by Z^+.

$S_1' \rightarrow S_1''$. An electron is transferred quickly from the [Mn(III)] to RAL^+: RAL–[Mn(IV)] is formed. In the case where RAL is a catechol, it has been shown (18, 19) that this process can also occur in aprotic media.

$S_1'' \rightarrow S_{1A}$. A H^+ is released easily from the H_2O ligand of (Mn) because of the unique property of Mn^{3+} mentioned under the justification of assumption 5. Then a H^+ in the H_2O molecule bound to A-[Mn(IV)] in S_1'' is transferred to the (Mn) complex along the hydrogen bond, producing the state S_{1A}. The proton transfer from [Mn(IV)]OH_2 to $(Mn)(OH)^-$ has a negative standard free energy (ΔF) and no energetic barrier, because of the following reason: generally a H^+ transfer along a hydrogen bond becomes easier, as the positive charge in the H^+ donor ([Mn(IV)]OH_2) and the negative charge in the H^+ acceptor [$(Mn)(OH)^-$] increase (30). Kusunoki *et al.* (31) have shown from quantum mechanical calculations that the H^+ transfer from [Mn(IV)]OH_2 to H_2O has a negative ΔF and no barrier. Since the H^+ acceptor, $(OH)^-$, in our model is more negative than H_2O, the H^+ transfer from S_1'' to S_{1A} should also be facilitated. Therefore, for the rapid and exothermal transfer of H^+, it is very important that the $(OH)^-$ ligand be stable in the (Mn) complex.

$S_{1A} \rightleftarrows S_{1B}$. An intramolecular electron transfer occurs between RAL and [Mn] in the A-[Mn] complex because the redox potential of RAL/RAL^+ is close to that of

Biochemistry: Kambara and Govindjee

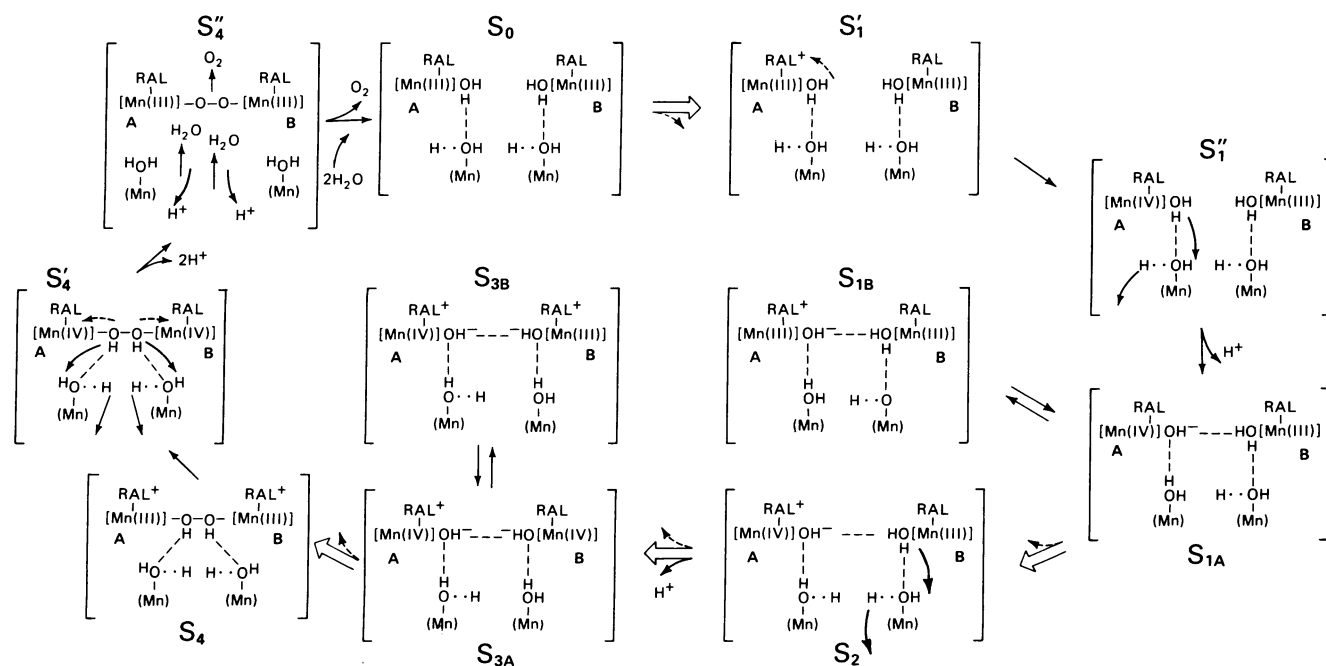Proc. Natl. Acad. Sci. USA 82 (1985)   6121

FIG. 2.   Model of the microscopic mechanism of H_2O oxidation in photosynthesis, described according to Kok's four-photon scheme of the redox cycle. (Mn) is always trivalent. The states with primes denote short-lived transition states. S_{1A} and S_{1B} (or S_{3A} and S_{3B}) are two equilibrium states. Open arrows mean photon absorption and dashed arrows mean transfer of electrons. For other abbreviations, see the legend of Fig. 1.

Mn(III)/Mn(IV) in catechol complexes (19, 32). An equilibrium exists between RAL·[Mn(IV)] and RAL$^+$·[Mn(III)]—that is, between S_{1A} and S_{1B}.

The Process for the $S_1 \rightarrow S_2$ Reaction. An electron is transferred from RAL of A-[Mn] in S_{1A} to Z^+ after the absorption of a second photon by P680, and S_2 is produced. The electron transfer in the $S_1 \rightarrow S_2$ reaction may be slower than in the $S_0 \rightarrow S_1$ reaction, because the electron transfer to Z^+ cannot occur from RAL$^+$ in S_{1B}. The electron distribution of the OH ligand in A-[Mn] becomes close to that of an OH· radical.

The Process for the $S_2 \rightarrow S_3$ Reaction. After the absorption of a third proton by P680, the electron donation to Z^+ must occur from RAL of B-[Mn]. The electron transfer in the reaction $S_2 \rightarrow S_3$ would be slower than that in $S_1 \rightarrow S_2$ because the distance to Z from B-[Mn] is longer than that from A-[Mn]; in addition, an excess positive charge exists in S_2 over that in S_1. The splitting of an OH bond in B-[Mn] and H$^+$ release occur in a manner similar to that in the $S_0 \rightarrow S_1$ reaction. The S_{3B} state coexists with S_{3A}.

The Process of the $S_3 \rightarrow S_4 \rightarrow S_0$ Reaction: $S_{3A} \rightarrow S_4$. After the absorption of a fourth photon by P680, an electron is transferred from RAL of B-[Mn] to Z^+. The electron transfer in $S_{3A} \rightarrow S_4$ would be slower than that in $S_2 \rightarrow S_{3A}$ because the probability that B-[Mn] is in S_{3A} is less than unity. The electron distribution of the OH ligand in B-[Mn] becomes close to that of an OH· radical. An "H_2O_2" intermediate is formed from the two OH· ligands (33), and the two [Mn] ions become trivalent. The two (Mn) complexes redistribute so as to form a more stable configuration, and new hydrogen bonds are formed between H_2O_2 and (Mn) complexes, since the OH bond axes in H_2O_2 are perpendicular to the O—O bond axis (34).

$S_4 \rightarrow S_4' \rightarrow S_4''$. An equilibrium exists between RAL$^+$·[Mn(III)] and RAL·[Mn(IV)] in both A- and B-[Mn] complexes. When both [Mn] complexes are in the RAL·[Mn(IV)] state at the same time, a double electron transfer occurs from H_2O_2 to the two [Mn(IV)] ions and 2H$^+$ are transferred to the relevant (Mn) complexes along the hydrogen bonds. Then, 2H$^+$ are released from the (Mn)

complexes. A realistic picture of the splitting of H_2O_2 into O_2 + 2H$^+$ can be obtained from the reaction of Mn^{3+} with H_2O_2 in aqueous media. Davies et al. (35) showed that the overall stoichiometry of the reaction of Mn^{3+} is: $2Mn^{3+} + H_2O_2 \rightleftharpoons 2Mn^{2+} + O_2 + 2H^+$. The overall rate-determining step in the above reaction is the electron transfer process from H_2O_2 to Mn^{3+} (35).

$S_4'' \rightarrow S_0$. After the 2H$^+$ are released, the two (Mn) complexes move out from the entrance of the cavity (see Fig. 1) and two H_2O molecules enter into the cavity. Then the O_2 molecules in the complex of Mn(III)–O_2–Mn(III) is replaced exothermally by the two H_2O molecules, since the binding energy of H_2O with Mn(III) (36) is much larger than that of O_2 (37). Hydrogen bonds are formed between [Mn] and (Mn) complexes, and the WOC returns to S_0.

JUSTIFICATION OF THE MODEL

We analyze the present model by describing the various predicted properties for the water oxidation system and comparing them with the available observed data. Results are summarized in Table 1.

Atomic Structure of WOC. The essential part of the WOC in the model is shown in Fig. 1. We speculate that the two Mn atoms that are in closer physical proximity to Z (21) and the two Mn atoms that are essential in restoring electron donation to P680 (12) may correspond to our two [Mn] atoms. The two loosely bound Mn atoms supported by the 33-kDa extrinsic protein (15, 17, 25) may correspond to our (Mn) atoms.

Electron Transfer. (i) In our model, the electron path from the WOC to Z^+ in $S_2 \rightarrow S_3$ and $S_3 \rightarrow S_4$ is different from the path in $S_0 \rightarrow S_1$ and $S_1 \rightarrow S_2$ (cf. refs. 29 and 38). (ii) The half-life of $t_{i,i+1}$ for electron transfer in $S_i \rightarrow S_{i+1}$ has the relation of $t_{0,1} < t_{1,2} < t_{2,3} < t_{3,4}$ in the model. (iii) It is expected that the value of $t_{1,2}/t_{0,1}$ is close to that of $t_{3,4}/t_{2,3}$, since the retardation of $t_{1,2}$ compared to $t_{0,1}$ arises from the same origin as that for $t_{3,4}$ compared to $t_{2,3}$. The closeness of the experimental values supports our model. (iv) We suggested that the rate-limiting step in each $S_i \rightarrow S_{i+1}$ transition

Table 1. Predictions and their possible relation to the observed results

Prediction	Experimental
Atomic structure of WOC	
RAL·[Mn]---(Mn)	Of the four functional Mn atoms, two
Z	couple with Z (12, 21)
RAL·[Mn]---(Mn)	and two are "loosely" bound (15, 17)
Electron transfer	

(i) Two different electron pathways from WOC to Z

$$\begin{array}{c} S_0,S_1 \rightarrow \text{RAL in A} \\ \text{WOC} \qquad\qquad\qquad Z \\ S_2,S_3 \rightarrow \text{RAL in B} \end{array} \qquad \begin{array}{c} S_0,S_1 \rightarrow Y_{0,1} \\ \text{WOC} \qquad\qquad\qquad Z \ (38) \\ S_2,S_3 \rightarrow Y_{2,3} \end{array}$$

(ii) Half-lives $T_{i,i+1}$ for electron transfer in $S_i \rightarrow S_{i+1}$

$T_{0,1} < T_{1,2} < T_{2,3} < T_{3,4}$	$T_{0,1}$ $T_{1,2}$ $T_{2,3}$ $T_{3,4}$
	30 μs 110 μs 350 μs 1.3 ms (39)

(iii) Ratio of the half-lives

$T_{1,2}/T_{0,1} \cong T_{3,4}/T_{2,3}$	$T_{1,2}/T_{0,1} = 3.7,$
	$T_{3,4}/T_{2,3} = 3.7$ (39)

(iv) The rate-limiting step in each $S_i \rightarrow S_{i+1}$ transition

The electron transfer from RAL to Z^+	The breaking of OH bonds is not the limiting step (40)

(v) The free energy difference ΔF for each $S_i \rightarrow S_{i+1}$ transition

$S_0 \rightarrow S_1$, $S_1 \rightarrow S_2$, $S_2 \rightarrow S_3$, $S_3 \rightarrow S_4$	$S_0 \rightarrow S_1$ $S_1 \rightarrow S_2$ $S_2 \rightarrow S_3$ $S_3 \rightarrow S_4$
$\Delta F_{0,1} \cong \Delta F_{1,2} \cong \Delta F_{2,3} \cong \Delta F_{3,4}$	(0.24) 0.89 0.93 0.87
	>0.5 — — (eV)
	(29, 41)

Charge on the WOC	

(i) Variation of the total charge on the WOC

$S_0 \rightarrow S_1$, $S_1 \rightarrow S_2$, $S_2 \rightarrow S_3$, $S_3 \rightarrow S_0$	$S_0 \rightarrow S_1$, $S_1 \rightarrow S_2$, $S_2 \rightarrow S_3$, $S_3 \rightarrow S_0$
0 +1 0 −1	0 +1 0 −1
	(42)

(ii) Redox transition causing the variation in the charge of the WOC

$S_0 \rightarrow S_1$, 1/2[Mn(III) → Mn(IV)]	Mn(III) → Mn(IV)
1/2[RAL → RAL$^+$]	
$S_1 \rightarrow S_2$, 1/2[Mn(III) → Mn(IV)]	RAL → RAL$^+$ Mn(III) → Mn(IV)
1/2[RAL → RAL$^+$]	
$S_2 \rightarrow S_3$, 1/2[Mn(III) → Mn(IV)]	Mn(III) → Mn(IV)
1/2[RAL → RAL$^+$]	
$S_3 \rightarrow S_0$, 3/2[Mn(IV) → Mn(III)]	RAL$^+$ → RAL 3[Mn(IV) → Mn(III)]
3/2[RAL$^+$ → RAL]	(43) (20)

(iii) Proton Release Pattern

$S_0 \rightarrow S_1$, $S_1 \rightarrow S_2$, $S_2 \rightarrow S_3$, $S_3 \rightarrow S_0$	$S_0 \rightarrow S_1$, $S_1 \rightarrow S_2$, $S_2 \rightarrow S_3$, $S_3 \rightarrow S_0$
1 0 1 2	1 0 1 2
	(44–46)

Microscopic Structure of WOC	
	S_0
2RAL·Mn(III), 2Mn(III)	4Mn(III) (HT + EPR; ref. 47)
	S_1
½[RAL$^+$·Mn(III) RAL·Mn(IV)]	Mn(II), Mn(III) [or 2Mn(III)]
RAL·Mn(III), 2Mn(III)	(XAES; ref. 11)
	2Mn(III) (EPR; ref. 48)
	Mn(IV), 3Mn(III) (HT + EPR; ref.47)
	S_2
RAL$^+$·Mn(IV), RAL·Mn(III)	Mn(IV), Mn(III) (XAES; ref. 11)
2Mn(III)	Mn(IV), 3Mn(III) (EPR; ref. 47)
	Mn(IV), Mn(III) (EPR; ref. 10)
	S_3
½[RAL$^+$·Mn(III) RAL·Mn(IV)]	2Mn(IV), 2Mn(III)
RAL$^+$·Mn(IV), 2Mn(III)	(HT + EPR; ref. 47)
	S_4
[RAL$^+$·Mn(III) RAL·Mn(IV)]	2Mn(IV), 2Mn(III) (HT + EPR; ref. 47)
2Mn(III)	

Effect of Cl$^-$	
Cl$^-$ participates in the water-splitting process by stabilizing (Mn(III)) ions in hydrophilic region	Cl$^-$ is essential for stabilizing the functional Mn complexes (5)
Upon Cl$^-$ depletion	
$S_1 \rightarrow S_2$ is not affected directly, but $S_0 \rightarrow S_1$, $S_2 \rightarrow S_3$, $S_3 \rightarrow S_4 \rightarrow S_0$ transitions become difficult	$S_1 \rightarrow S_2$ is not affected, but $S_2 \rightarrow S_3$ is prevented (49, 50)

Numbers in parentheses are references. HT + EPR, EPR of heat-treated sample.

is the electron transfer from RAL to Z^+: In $S_0 \rightarrow S_1$, the proton transfer is expected to be quicker than the intermolecular electron transfer from RAL to Z^+, since there is no potential barrier along the proton transfer path. The situation in $S_2 \rightarrow S_3$ is almost the same as in $S_0 \rightarrow S_1$. In $S_3 \rightarrow S_4$, the formation of H_2O_2 from 2OH radicals should be

faster than the intermolecular electron transfer (33), since the 2OH radicals are kept close to each other and the formation of "H_2O_2" is exothermic. (v) The ΔF for the $S_i \rightarrow S_{i+1}$ transition kinetics arises mainly from the energy difference between the initial state, RAL·Z^+, and the final state, RAL$^+$·Z, because the rate-limiting process in each $S_i \rightarrow S_{i+1}$ transition is the electron transfer from RAL to Z^+. Therefore, the values of ΔF for the four $S_i \rightarrow S_{i+1}$ steps are expected to be close to each other. The value of 0.24 eV for $S_1 \rightarrow S_2$ was estimated only from the back reaction, $S_1 \rightarrow S_0$ (29), which cannot be the same for the $S_0 \rightarrow S_1$ reaction; the estimate of >0.5 eV (41) seems to us to be more reliable. Thus, the ΔF values for all the steps are similar.

Charge on the WOC. The redox transition causing the variation in the charge of the WOC in each transition $S_i \rightarrow S_{i+1}$ is derived from the difference in the microscopic state of the WOC between the S_i and S_{i+1} states (Fig. 2). The $S_0 \rightarrow S_1$, $S_1 \rightarrow S_2$, $S_2 \rightarrow S_3$, and $S_3 \rightarrow S_0$ transitions are all characterized by the same difference absorbance spectrum, with an amplitude change of +1, +1, +1, and −3, respectively (20). It seems that the oxidation of a Mn(III) to Mn(IV) is involved in the $S_0 \rightarrow S_1$, $S_1 \rightarrow S_2$, and $S_2 \rightarrow S_3$ transitions, and the reduction of three Mn(IV) ions occurs in $S_3 \rightarrow S_0$. These results are also predicted from our model. If the population probability of RAL·[Mn(IV)] in S_{1A} (S_{3A}) is comparable to that of RAL$^+$·[Mn(III)] in S_{1B} (S_{3B}), then the contribution of RAL → RAL$^+$ to the redox transition in the WOC is nearly equal in each $S_i \rightarrow S_{i+1}$ step, and that of Mn(III) → Mn(IV) is also constant in each step. Thus, the amplitude sequence of +1, +1, +1, −3 in the difference spectrum is expected from our model, although it does not correspond to the pure Mn(III) → Mn(IV) transition but to the mixture of Mn(III) → Mn(IV) and RAL → RAL$^+$ transitions. The nearly equal population of S_{1A} and S_{1B} and of S_{3A} and S_{3B} is reasonable because $t_{0,1}/t_{1,2}$ and $t_{2,3}/t_{3,4}$ are approximately equal to the probability of RAL·[Mn(IV)] in S_1 and S_3, respectively and their value is >1/4. Finally, the H$^+$ release pattern in the model is consistent with the available data.

The Microscopic Structure of the WOC in Each S State. This is described by the electronic structure of the A-[Mn], B-[Mn], and two (Mn) complexes (Fig. 2; Table 1). The assignments of the electronic states of the Mn ions by x-ray absorption edge spectra (XAES; ref. 11), EPR at low temperature (10, 47, 48), and EPR for heat-treated samples (47) are consistent with the model. Goodin *et al.* (11) suggested two possible structures, Mn(II)·Mn(III) and 2 Mn(III), for S_1. The present model favors the latter structure.

Effect of Cl$^-$ Ions. A major effect of Cl$^-$ depletion in the model is that protons transferred from the [Mn] to the (Mn) complex would not be released smoothly to the lumen because Cl$^-$ depletion changes (Mn(III)) into (Mn(II)) (26), and the equilibrium constant for Mn(II)OH$_2 \rightleftharpoons$ Mn(II)OH$^-$ + H$^+$ in aqueous media is quite small compared with that for Mn(III) (51). Since it is difficult for the (Mn) complex to accept a H$^+$ from the [Mn] complex, the transitions $S_0 \rightarrow S_1$, $S_2 \rightarrow S_3$, and $S_3 \rightarrow S_4$ would be difficult in Cl$^-$-depleted samples. However, the $S_1 \rightarrow S_2$ transition is not directly affected by Cl$^-$ depletion because this transition is not associated with the proton transfer. This is consistent with the observed results (49, 50).

CONCLUDING REMARKS

Our model (Figs. 1 and 2) is consistent with all known aspects of electron transfer from H_2O to Z (Table 1). We have tentatively considered catechol as the RAL, in order to describe the model concretely. However, there is no evidence for catechol to be a component of PSII. (PQ) is a candidate for RAL, but the number of PQ molecules in PSII

might not be enough: at least five PQ molecules (2 RAL, 1Z, 1Q$_A$ and 1Q$_B$), are required for our model, but the reported number is about 3.5 (13). Another possible candidate is histidine or tyrosine: it may coordinate to the [Mn] ion (52). A stable free radical of an aromatic amino acid has been reported to exist near the heme in cytochrome *c* peroxidase (53). Thus, we propose that one of the aromatic amino acids may carry out the function of RAL.

1. Govindjee, Kambara, T. & Coleman, W. (1985) *Photochem. Photobiol.*, in press.
2. Joliot, P. & Kok, B. (1975) in *Bioenergetics of Photosynthesis*, ed. Govindjee (Academic, New York), pp. 387–412.
3. O'Malley, P. J. & Babcock, G. T. (1984) *Biochim. Biophys. Acta* 765, 370–379.
4. Amesz, J. (1983) *Biochim. Biophys. Acta* 726, 1–12.
5. Izawa, S., Muallem, A. & Ramaswamy, N. K. (1983) in *Oxygen Evolving System of Photosynthesis*, eds. Inoue, Y., Crofts, A. R., Govindjee, Murata, N., Renger, G. & Satoh, K. (Academic, Tokyo), pp. 293–302.
6. Renger, G. (1977) *FEBS Lett.* 81, 223–228.
7. Govindjee, Wydrzynski, T. & Marks, S. B. (1977) in *Bioenergetics of Membranes*, eds. Packer, L., Papageorgiou, G. & Trebst, A. (Elsevier-North Holland, Amsterdam), pp. 305–316.
8. Lawrence, G. D. & Sawyer, D. T. (1978) *Coord. Chem. Rev.* 27, 173–193.
9. Wydrzynski, T. & Sauer, K. (1980) *Biochim. Biophys. Acta.* 589, 56–70.
10. Andreasson, L. E., Hansson, O. & Vänngard, T. (1983) *Chem. Scr.* 21, 71–74.
11. Goodin, D. B., Yachandra, V. K., Britt, R. D., Sauer, K. & Klein, M. P. (1984) *Biochim. Biophys. Acta* 767, 209–216.
12. Klimov, V. V., Allakhverdiev, S. I., Shuvalov, V. A. & Krasnovskii, A. A. (1982) *FEBS Lett.* 148, 307–312.
13. Murata, N., Miyao, M., Omata, T., Matsunami, H. & Kuwabara, T. (1984) *Biochim. Biophys. Acta* 765, 363–369.
14. Bishop, N. I. (1984) in *Advances in Photosynthesis Research*, ed. Sybesma, C. (Nijhoff, The Hague), Vol. 1, pp. 321–328.
15. Ono, T. & Inoue, Y. (1984) *FEBS Lett.* 168, 281–286.
16. Metz, J. G., Wong, J. & Bishop, N. I. (1980) *FEBS Lett.* 114, 61–66.
17. Miyao, M. & Murata, N. (1984) *FEBS Lett.* 170, 350–354.
18. Magers, K. D., Smith, C. G. & Sawyer, D. T. (1978) *J. Am. Chem. Soc.* 100, 989–991.
19. Lynch, M. W., Hendrickson, D. N., Fitzgerald, B. J. & Pierpont, C. G. (1984) *J. Am. Chem. Soc.* 106, 2401–2409.
20. Dekker, J. P., van Gorkom, H. J., Wensink, J. & Ouwehand, L. (1984) *Biochim. Biophys. Acta* 767, 1–9.
21. Yocum, C. F., Yerkes, C. T., Blankenship, R. E., Sharp, R. R. & Babcock, G. T. (1981) *Proc. Natl. Acad. Sci. USA* 78, 7507–7511.
22. Ghanotakis, D. F., Babcock, G. T. & Yocum, C. F. (1984) *Biochim. Biophys. Acta* 765, 388–398.
23. Villafranca, J. J., Yost, F. J. & Fridovich, I. (1974) *J. Biol. Chem.* 249, 3532–3536.
24. Radmer, R. & Ollinger, O. (1983) *FEBS Lett.* 152, 39–43.
25. Seibert, M. & Cotton, T. (1985) *FEBS Lett.* 182, 34–38.
26. Davies, G. (1969) *Coord. Chem. Rev.* 4, 199–224.
27. Wells, C. F. (1965) *Nature (London)* 205, 693–694.
28. Nagle, J. F. & Nagle, B. (1983) *J. Membr. Biol.* 74, 1–14.
29. Bouges-Bocquet, B. (1980) *Biochim. Biophys. Acta* 594, 85–103.
30. Brickman, J. (1976) in *The Hydrogen Bond*, eds. Schuter, P., Zundel, G. & Sandorfy, C. (North Holland, Amsterdam) Vol. 1, pp. 217–244.
31. Kusunoki, M., Kitaura, K., Morokuma, K. & Nagata, C. (1980) *FEBS Lett.* 117, 179–182.
32. Magers, K. D., Smith, C. G. & Sawyer, D. T. (1980) *Inorg. Chem.* 19, 492–496.
33. Taube, H. (1970) *Electron Transfer Reaction of Complex Ions in Solution* (Academic, New York).
34. Stevens, R. M. (1970) *J. Chem. Phys.* 52, 1397–1402.
35. Davies, G., Kirschenbau, L. J. & Kustin, K. (1968) *Inorg. Chem.* 7, 146–154.
36. Zhogolev, D. A., Bunyatyan, B. Kh., Volkov, V. B. & Yatsimivskii, K. B. (1974) *Chem. Phys. Lett.* 29, 506–511.
37. Coleman, W. M. & Taylor, L. T. (1978) *Inorg. Chim. Acta* 30, L291–L293.
38. Boska, M. & Sauer, K. (1984) *Biochim. Biophys. Acta* 765, 84–87.
39. Dekker, J. P., Plijter, J. J., Ouwehand, L. & van Gorkom, H. J. (1984) *Biochim. Biophys. Acta* 767, 176–179.
40. Sinclair, J. & Arnason, T. (1974) *Biochim. Biophys. Acta* 368, 393–400.
41. Kok, B., Radmer, R. & Fowler, C. F. (1975) *Proc. Int. Congr. Photosynth.* 485–496.
42. Saygin, O. & Witt, H. T. (1984) *FEBS Lett.* 176, 83–87.
43. Velthuys, B. R. (1981) in *Photosynthesis*, ed. Akoyunoglou, G. (Balaban Science, Philadelphia), Vol. 2, pp. 75–85.
44. Fowler, C. F. (1977) *Biochim. Biophys. Acta* 462, 414–421.
45. Saphon, S. & Crofts, A. R. (1977) *Z. Naturforschg. C. Biosci.* 32C, 617–626.
46. Förster, V., Hong, Y.-Q. & Junge, W. (1981) *Biochim. Biophys. Acta* 638, 141–152.
47. Dismukes, G. C., Ferris, K. & Watnick, P. (1982) *Photobiochem. Photobiophys.* 3, 243–256.
48. Abramowicz, D. A., Raab, T. K. & Dismukes, G. C. (1984) in *Advances in Photosynthesis Research*, ed. Sybesma, C. (Nijhoff, The Hague), Vol. 1, pp. 349–353.
49. Itoh, S., Yerkes, C. T., Koike, H., Robinson, H. H. & Crofts, A. R. (1984) *Biochim. Biophys. Acta* 766, 612–622.
50. Theg, S. M., Jursinic, P. & Homman, P. H. (1984) *Biochim. Biophys. Acta* 766, 636–646.
51. Wells, C. F. & Davies, G. (1967) *J. Chem. Soc. A*, 1858–1861.
52. Sundberg, R. J. & Martin, R. B. (1974) *Chem. Rev.* 74, 471–517.
53. Coulson, A. F. W. & Yonetani, T. (1972) *Biochem. Biophys. Res. Commun.* 49, 391–398.